Shear-Induced Diffusion of Platelike Particles in Microchannels

Roberto Rusconi and Howard A. Stone

School of Engineering and Applied Sciences, Harvard University, Cambridge, Massachusetts, USA

(Received 30 July 2008; published 16 December 2008)

We exploit the recent developments of microfluidic technologies to investigate the collective shear-induced diffusion in suspensions of micron-sized particles. Whereas spherical particles do not diffuse on the time scale of our experiments, the results with platelike clay particles show a strong cross-stream shear-induced diffusivity at low volume fraction ($\phi_0 \leq 0.01$). Moreover, we find a linear dependence of the collective diffusion coefficient with the average shear rate (in the range 10^2–10^4 s^{-1}) and the particle concentration. These data are in good agreement with previous experimental and theoretical results for spheres when rescaled with the particle number density.

DOI: 10.1103/PhysRevLett.101.254502 PACS numbers: 47.61.−k, 83.50.Ax, 87.16.dp

Shear-induced diffusion (SID) refers to the effective diffusive motion of particles in a shear flow, which increases as the shear rate of the suspending fluid increases. This phenomenon stems from hydrodynamic or other interactions among neighboring particles, induced by the different relative speed along streamlines, which can produce displacements from the average trajectories, even in the direction perpendicular to the velocity gradient. The resulting irregular motion of a tagged particle can then be interpreted as a random walk characterized by a self-diffusion coefficient, D^s, which, at low Reynolds numbers, scales, by dimensional analysis, as $D^s = \dot{\gamma} R^2 f_s(\phi)$, where R is the particle radius, $\dot{\gamma}$ is the local shear rate, and $f_s(\phi)$ is a function of the particle volume fraction ϕ [1,2]. Similar to quiescent dispersions, a sheared suspension of an inhomogeneous distribution of particles produces a flux, $\mathbf{J}$, which can be expressed as

$$\mathbf{J} = -D^c(\phi)\nabla\phi, \tag{1}$$

where $D^c = \dot{\gamma} R^2 f_c(\phi)$ is the collective (or gradient) SID coefficient, with $f_c > f_s$ [3]. Moreover, due to the directionality of the flow, these coefficients are anisotropic: the diffusivity in the plane of shear is larger by about a factor of 1.5–2 than that in the vorticity direction [4,5].

Most of the previous experimental investigations [6–9] have been performed on concentrated suspensions of noncolloidal spheres using cylindrical Couette devices. There are only a few measurements of SID coefficient in dilute dispersions [10] and Brownian particles [11] available in the literature, since in these conditions the diffusivity is usually very small. Recently, Lopez and Graham [12] showed, via numerical simulations, that rods and branched particles can have shear-induced diffusivities much larger than those of spheres. In this Letter, we present experimental investigations of the cross-stream collective SID in dispersions (volume fraction $\phi_0 \leq 0.01$) of micron-sized platelike particles, and report much larger values (about 2 orders of magnitude) of the diffusivity than those obtained for sheared suspensions of spheres in the same range of volume fraction.

Our experimental setup is based on a microfluidic T sensor [13,14], which consists, in its simplest configuration, of two fluids entering through separate inlets and merging to flow side by side. Since the flow in uniform smooth microfluidic channels is laminar without mixing between the streamlines, in steady conditions the only possibility to allow mass transport transverse to flow direction is by diffusion. This T-sensor approach, indeed, can be a very efficient method to separate large and small molecules according to their different sizes and diffusivities. Here we used this device to measure the SID by flowing a particle suspension in one inlet and a pure solvent in the second inlet. Spreading of the concentration profile transverse to the flow direction then gives a measure of the shear-induced diffusivity. The layout of the mask used to make the microfluidic channels is displayed in Fig. 1(a). The typical width W of the channel used in the experiments is 200 μm, and we prepared different channels with various heights H ranging from 8 to 18 μm, whose uniformity have been checked by profilometry. Since $W \gg H$, the fully developed velocity profile is parabolic across the shortest direction and approximately uniform in the larger cross-sectional direction [Fig. 1(b)].

We define the coordinate system so that the migration of the particles is in the x direction, the flow is in the y direction, and the predominant shear is in the z direction. The channels were made in polydimethylsiloxane and then sealed to a glass microscope slide using standard soft-lithography techniques [15]. In order to measure small diffusivities we prepared channels with a very long length, $L = 50$ cm, by designing a series of turns with radius of curvature of 400 μm. One of the advantages of a microfluidic experiment is the chance to apply a wide range of flow rates: in this case $v = 1$–64 mm/s, where v is the mean velocity in the channel. By changing v and using channels with different heights, we were able to vary the mean shear rate, given by $\dot{\gamma} = 3v/H$, in the range 10^2–10^4 s^{-1}, which are much higher values than those typically obtained in Couette devices.

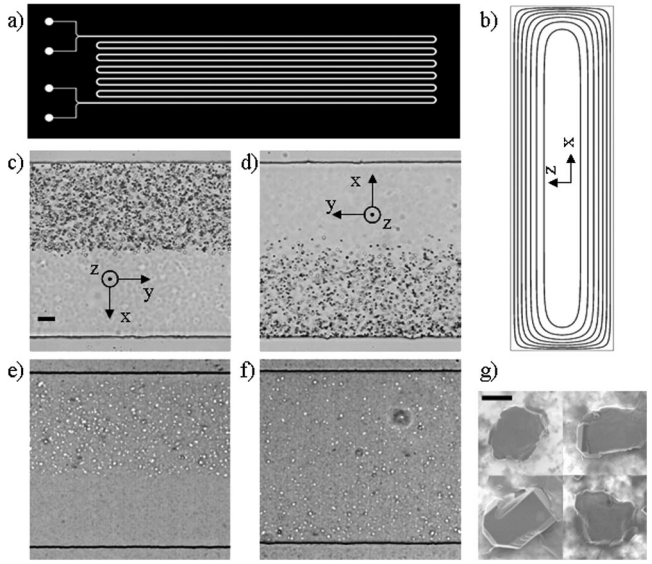

FIG. 1. (a) Schematic of the microfluidic device used in the experiments: the width of the channel is 200 μm and the overall length is 50 cm. (b) Velocity distribution for a pressure-driven flow through a rectangular cross section in case of an aspect ratio H/W between the height and the width of the channel of 0.1 (not to scale). (c)–(f) Bright-field microscopy images of a 13 μm-high channel (the scale bar is 20 μm) at (c),(e) the inlet and (d),(f) the outlet, for suspensions of (c),(d) polystyrene spheres (volume fraction $\phi_0 = 0.01$) and (e),(f) clay particles (white dots, $\phi_0 = 0.0075$): whereas the spheres do not migrate, the platelike particles are dispersed throughout the whole width of the channel. (g) SEM images of the clay particles (the scale bar is 1 μm).

The channel Reynolds number and the particle Reynolds number, defined, respectively, as $\mathrm{Re}_c = \rho v d_h/\eta$ and $\mathrm{Re}_p = \mathrm{Re}_c(2R/d_h)^2$, where d_h is the hydraulic diameter of the channel, ρ and η are, respectively, the density and the dynamic viscosity of the fluid, fall in the range $\mathrm{Re}_c \approx 0.01$–1 and $\mathrm{Re}_p \approx 5 \times 10^{-5}$–$5 \times 10^{-3}$ for particles with radius $R \approx 1$ μm. Owing to these values of Re_p we can therefore neglect inertial effects or lift forces acting on the particle, which arise due to the interactions with the wall or due to curving channels. We also used straight and thicker channels ($H = 37$ μm) to compare the results and confirm our assumptions. Moreover, although the particle we used are colloidal, the Brownian diffusion cannot be observed on the time scale of our experiments since the Péclet number $\mathrm{Pe} = v(W^2/L)/D_B \gg 1$, where $D_B = k_B T/(6\pi\eta R)$ is the Brownian diffusion coefficient.

We first tested the setup using dilute dispersions of negatively charged spheres (White Sulfate Latex, IDC), with a radius $R = 0.8$ μm and a volume fraction $\phi_0 = 0.01$–0.05. Figures 1(c) and 1(d) clearly show that these particles do not diffuse across the streamlines for the time it takes to cover the entire length of the channel (less than 100 s). The SID, at least in this range of ϕ, is thus too small to be observed ($D < 1$ μm^2/s). The experiment also makes clear that the Brownian motion does not produce any noticeable effect.

We then used dispersions of micron-sized clay platelets (SWy-2 montmorillonite, Wyoming). These particles, at $p\mathrm{H} > 7$, are slightly but uniformly negatively charged and can form stable dispersions for volume fractions up to 3% [16]. All the samples used in the experiments have been prepared diluting a single mother batch of $\phi_0 = 0.01$ in a sodium tetraborate/hydrochloric acid buffer ($p\mathrm{H} = 8$) and filtered several times using 3.1 μm filters. The volume fraction of the batch has been calculated by measuring the density of the sample and using the tabulated value for the density of montmorillonite, which is 2.33 g/cm^3. The solutions remained stable for months with no indication of aggregation or transition to the gel phase. Furthermore, we have performed experiments by adding to the suspensions up to 200 mM of NaCl to screen the electrostatic repulsion between the particles, but we did not observe any significant difference in the results.

Microscope images of the flowing suspensions of clay particles are displayed in Figs. 1(e) and 1(f). The density profile in the transverse direction is measured by counting all of the particles in a square field of view, 200 μm $\times$ 200 μm, and averaging over 100 images taken every 0.2 s, after subtraction of the background. Using a much higher acquisition rate (around 3000 frames per second) it is also possible to track the movement of every detected particle to obtain a direct measurement of the average speed of the

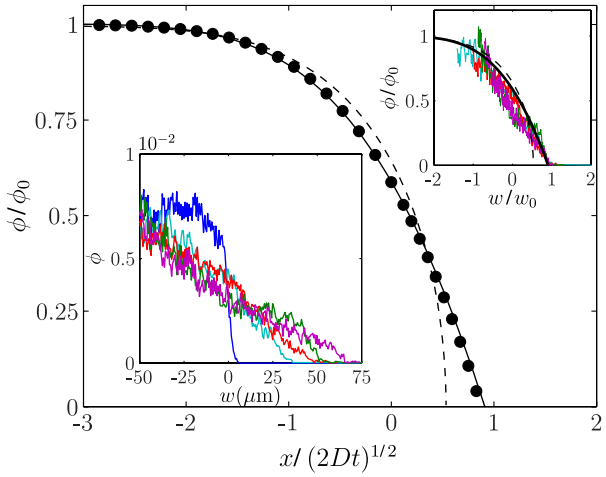

FIG. 2 (color online). Main: Numerical solution of Eq. (3) with $m = 1$ (solid line) and $m = 2$ (dashed line). The full circles (●) represent the numerical simulation for the 2D problem in the case of linear dependence on the volume fraction ($m = 1$). Lower left-hand inset: Particle concentration profiles (13 μm-high channel, $v = 12.8$ mm/s, $\phi_0 = 0.0075$) at incremental positions ℓ along the channel, i.e. (from left to right), $\ell = 0$ (inlet), $\ell = 85$ mm, $\ell = 167.5$ mm, $\ell = 250$ mm, $\ell = 332.5$ mm. Upper right-hand inset: All the experimental curves rescaled with the instantaneous profile width, w_0. The thick solid curve and the dashed curve are, respectively, the numerical solutions of Eq. (3) with $m = 1$ and with $m = 2$.

flow. Furthermore, via image analysis, we estimated the "effective" average radius $R \approx 0.8 \pm 0.2$ μm. The thickness of the particles, $h \approx 28 \pm 8$ nm, has been measured using a profilometer (with a vertical resolution of 1 nm) after deposition on a silicon wafer. These values are in good agreement with scanning electron microscopy (SEM) images of the particles [Fig. 1(g)]. In addition, an estimate of the sedimentation velocity for a disk with aspect ratio $r = h/2R \approx 0.0175$ gives $v_s \approx 50$ nm/s, which means that the settling is negligible on the time scale of our experiments.

The lower left-hand inset of Fig. 2 displays the experimental spreading of the particle concentration profile measured at different positions along the channel. The profile width is directly related to the effective diffusion coefficient, but the exact relationship can be found only by solving the appropriate diffusion equation. Considering a one-dimensional problem, the diffusion equation is given by

$$\frac{\partial \phi}{\partial t} = \frac{\partial}{\partial x}\left[D_0 \phi^m \left(\frac{\partial \phi}{\partial x}\right)\right], \tag{2}$$

where $\phi = \phi(x, t)$ is the particle volume fraction and m is an arbitrary exponent that characterizes the transverse shear-induced diffusive process. The boundary conditions are $\phi \to \phi_0$ for $x \to -\infty$ and $\phi \to 0$ for $x \to +\infty$, where ϕ_0 is the initial volume fraction. The initial condition is $\phi(x, 0) = \phi_0$ for $x \leq 0$ and $\phi(x, 0) = 0$ for $x > 0$. It is possible, via applying the transformation $\psi(\eta) = \phi/\phi_0$ and $\eta = x/(2D_0\phi_0^m t)^{1/2}$, to reduce Eq. (2) to the ordinary differential equation

$$-\eta\psi' = (\psi^m \psi')', \tag{3}$$

which can be solved numerically (Fig. 2). We also performed finite-element numerical simulations of the two-dimensional problem, i.e., a section of the channel perpendicular to the flow, in which the dependence of D_0 on the shear rate in the z direction has been considered: we found that the lateral diffusion is only slightly affected by the nonuniform shear in the channel, since the concentration profile rapidly equilibrates in the shortest direction. Moreover, the average profile along the z axis, which we observe with the microscope, is exactly the same as the one-dimensional problem (Fig. 2). We define η_0 according to $\psi(\eta_0) = 0.05$ and the profile width $w_0 = \eta_0(2Dt)^{1/2}$, with $D = D_0\phi_0^m$. In case of $m = 1$, we find numerically $\eta_0 \simeq 0.85$ and therefore $w_0 \simeq 1.2(Dt)^{1/2}$. All the experimental profiles, rescaled with the corresponding w_0, fall almost on the same curve, which is close to the numerical result for $m = 1$ (upper right-hand inset of Fig. 2). Thus, the data are consistent with a shear-induced diffusion coefficient that is linear in ϕ_0.

The linear dependence of the profile width w_0 with $t^{1/2}$, which we could expect from a diffusive behavior, has been verified in all the experiments performed for different values of the volume fraction and mean shear-rate (Fig. 3). Moreover, the diffusion coefficient D, determined

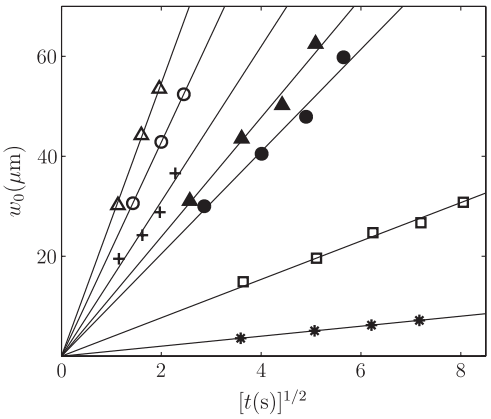

FIG. 3. Measured profile width w_0 as a function of time for different conditions of shear rate and particle concentration: (*) $\phi_0 = 0.0015$, $H = 13$ μm, $v = 6.4$ mm/s; (□) $\phi_0 = 0.00375$, $H = 13$ μm, $v = 6.4$ mm/s; (●) $\phi_0 = 0.005$, $H = 8$ μm, $v = 10.4$ mm/s; (▲) $\phi_0 = 0.0075$, $H = 13$ μm, $v = 12.8$ mm/s; (+) $\phi_0 = 0.0025$, $H = 13$ μm, $v = 64.1$ mm/s; (○) $\phi_0 = 0.005$, $H = 8$ μm, $v = 41.6$ mm/s; (△) $\phi_0 = 0.0075$, $H = 13$ μm, $v = 64.1$ mm/s.

by the linear fit $w_0 \simeq 1.2(Dt)^{1/2}$, is in turn directly proportional to the mean shear rate in the entire range of $\dot{\gamma}$ and for every particle concentration (Fig. 4). One significant consequence of the linear dependence of D with $\dot{\gamma}$ is that the profile spreading, at a given position ℓ along the channel, is independent of the mean speed v (Fig. 4, inset), since $w_0^2 \approx Dt \approx \dot{\gamma}t \approx (v/H)(\ell/v) \approx \ell/H$.

Finally, we can analyze the dependence on ϕ of the dimensionless coefficient $D/\dot{\gamma}R^2$, obtained by the linear fit with the shear rate of the experimental data. A pure hydrodynamic collision between two perfectly smooth noncolloidal spheres, owing to the linearity and time reversibility of the Stokes flow, is symmetrical: the particles return to their original streamlines after the passing encounter. Thus, at least three spheres must interact to have a net displacement, and consequently the diffusivity is expected to scale as ϕ^2. Instead, the presence of irreversibilities [17], due to nonhydrodynamic interactions such as repulsive forces or particle roughness, or symmetry breaking, as in the case of nonspherical particles, lead to a diffusivity which is predicted to be linear in ϕ in the dilute limit [12]. As shown in Fig. 5, our experimental data for the collective diffusion coefficient are very well fit by the linear function $D/\dot{\gamma}R^2 = 6.9\phi$. Moreover, these values of the shear-induced diffusivity are about 2 orders of magnitude larger than experimental data for dispersions of spheres at low volume fraction (Fig. 5, upper left-hand inset), which is in agreement with what we observed with spherical particles. However, since axisymmetric particles suspended in shear flows undergo tumbling motions, known as Jeffery orbits [18,19], with angular velocity $\omega \approx r\dot{\gamma}$, the effective volume spanned by the particles is much larger than the real one. Indeed, if we compare our results as a function of the particle number density $n = \phi/V_p$, where V_p is the vol-

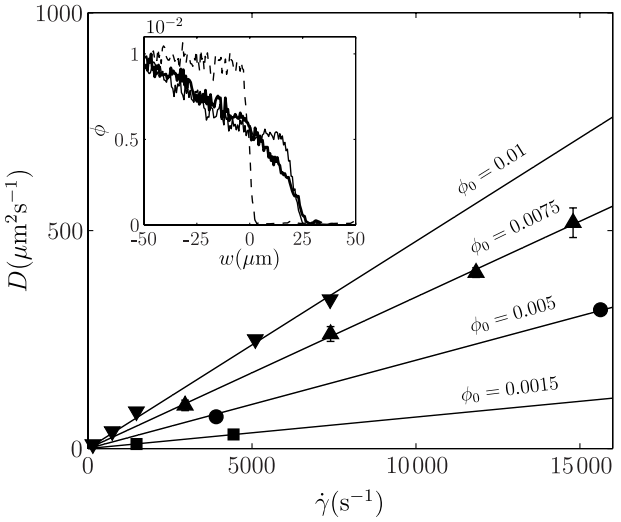

FIG. 4 (color online). Main: Linear dependence of the shear-induced diffusion coefficient on the mean shear rate for different initial particle concentrations. Inset: Comparison between the initial distribution of particles (dotted curve) and the concentration profiles at the same position along the channel ($\ell = 43.3$ mm) for $v = 0.9$ mm/s (thick solid curve) and $v = 9.2$ mm/s (solid curve).

ume of the particles, with theoretical [3] and experimental [7] data for the shear-induced collective diffusivity in concentrated suspensions of spheres (in the vorticity and velocity gradient direction, respectively), we obtain a good qualitative agreement (Fig. 5, lower right-hand inset).

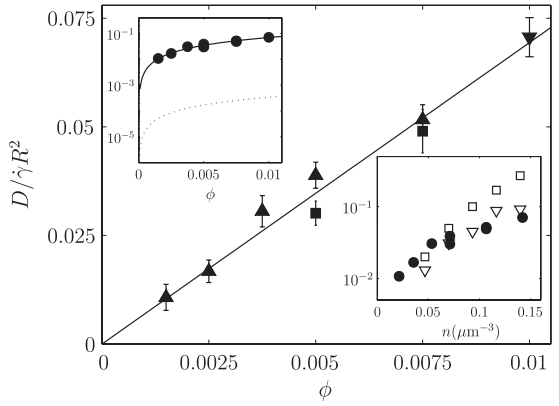

FIG. 5. Main: Linear dependence of the dimensionless shear-induced diffusivity on the volume fraction. Each point has been obtained from the linear fit with the shear rate for all the collected data with different channel heights, i.e., 8 μm (■), 13 μm (▲), 10 and 18 μm (▼). Upper left-hand inset: Semilogarithmic plot of the same data in comparison with (dotted line) the function, $f(\phi) = 0.034\phi + 1.15\phi^3$, used to fit experimental data, for the self-diffusion coefficient within the plane of shear, in dilute dispersions of spheres [10]. Lower right-hand inset: Our data (●) as a function of the particle number density n in comparison with experimental (□) [7] and theoretical (▽) [3] results for collective diffusion in concentrated suspensions of spheres.

In summary, we propose a new experimental method, using a microfluidic device, to investigate the cross-stream collective SID of micron-sized particles. This technique gives precise and quantitative results over a wide range of shear rates and particle concentrations. We measured the SID in dispersions of platelike clay particles. Our results show a clear linear dependence with the mean shear rate and the particle volume fractions. The values of the dimensionless SID coefficient we obtained are about 2 orders of magnitude higher than those for spherical particles in the same range of volume fraction. Moreover, the diffusivity of these particles, when strongly sheared, can be enhanced by several orders of magnitude with respect to their Brownian diffusion. This result can be extremely important for many applications in microfluidic systems, as a way, for instance, to enhance transport and mixing [20] in suspensions of cells and macromolecules.

The authors acknowledge Jeff Morris for his insightful comments.

[1] E. C. Eckstein, D. G. Bailey, and A. H. Shapiro, J. Fluid Mech. **79**, 191 (1977).
[2] D. Leighton and A. Acrivos, J. Fluid Mech. **181**, 415 (1987).
[3] A. M. Leshansky, J. F. Morris, and J. F. Brady, J. Fluid Mech. **597**, 305 (2008).
[4] I. E. Zarraga and D. T. Leighton Jr, Phys. Fluids **13**, 565 (2001).
[5] G. Drazer, J. Koplik, B. Khusid, and A. Acrivos, J. Fluid Mech. **460**, 307 (2002).
[6] D. Leighton and A. Acrivos, J. Fluid Mech. **177**, 109 (1987).
[7] R. J. Phillips, R. C. Armstrong, R. A. Brown, A. L. Graham, and J. R. Abbott, Phys. Fluids A **4**, 30 (1992).
[8] S. I. Madanshetty, A. Nadim, and H. A. Stone, Phys. Fluids **8**, 2011 (1996).
[9] V. Breedveld, D. van den Ende, M. Bosscher, R. J. J. Jongschaap, and J. Mellema, Phys. Rev. E **63**, 021403 (2001).
[10] I. E. Zarraga and D. T. Leighton Jr, Phys. Fluids **14**, 2194 (2002).
[11] X. Qiu, H. D. Ou-Yang, D. J. Pine, and P. M. Chaikin, Phys. Rev. Lett. **61**, 2554 (1988).
[12] M. Lopez and M. D. Graham, Phys. Fluids **19**, 073602 (2007).
[13] B. H. Weigl and P. Yager, Science **283**, 346 (1999).
[14] A. E. Kamholz, E. A. Schilling, and P. Yager, Biophys. J. **80**, 1967 (2001).
[15] D. C. Duffy, J. C. McDonald, O. J. A. Schueller, and G. M. Whitesides, Anal. Chem. **70**, 4974 (1998).
[16] E. Tombácz and M. Szekeres, Appl. Clay Sci. **27**, 75 (2004).
[17] D. J. Pine, J. P. Gollub, J. F. Brady, and A. M. Leshansky, Nature (London) **438**, 997 (2005).
[18] G. B. Jeffery, Proc. R. Soc. A **102**, 161 (1922).
[19] K. Yasuda, M. Nishimura, and K. Chiba, J. Textil. Eng. **52**, 165 (2006).
[20] M. Lopez and M. D. Graham, Phys. Fluids **20**, 053304 (2008).